Proceedings of ASME Turbo Expo 2011
GT2011
June 6-10, 2011, Vancouver, British Columbia, Canada

GT2011-46668

IMPACT OF INTER-STAGE DYNAMICS ON STALLING STAGE IDENTIFICATION

Manuj Dhingra*
J.V.R. Prasad
Department of Aerospace Engineering
Georgia Institute of Technology
Atlanta, GA 30332-0150

Prashant Tiwari
GE Global Research Center
Niskayuna, NY 12309

Tsuguji Nakano
Andy Breeze-Stringfellow
GE Aviation
Cincinnati, OH 45215

ABSTRACT

A key objective of compressor rig tests is the identification of compressor stall boundary. A complementary goal is the identification of the stalling stage based on test data. This serves two purposes: 1) Validate the pre-test prediction of the stage loading distribution, and 2) identify the weak stages, should improvements in operating range be desired in subsequent design iterations. Typically the pertinent test data is in the form of static pressure measurements. Many engineers believe that a stalling stage is accompanied by a transient upstream pressure rise coupled with a downstream pressure loss. However, inter-stage dynamics may cloud the identification of the stalling stage. To this end, an analysis of inter-stage dynamics, immediately preceding the stall event, could provide an alternate assessment of the stalling stage. This work reviews existing stall models for studying compressor dynamics. The main focus of this work is to develop ability to capture inter-stage dynamics. A 3-state equation lumped Moore-Greitzer (MG3) model is widely used to study the dynamic compressor response during surge and rotating stall transients. However the evolution of MG3 model may not provide a suitable framework for the investigation of inter-stage dynamics. On the other hand, an unsteady time marching 1-D fluid dynamic model (e.g. similar to the DynTECC formulation which includes body forces), while unable to capture the rotating stall dynamics, is sufficient for this purpose. A numerical simulation has been developed to investigate the impact of stage characteristics, as well as load distribution on the compression and expansion waves that develop prior to a surge event. Through a controlled weakening of selected stages, the time evolution of these waves is related back to the stalling stage. It is found that the weakened stage is not necessarily the stalling stage as identified via the pressure rise and downstream pressure drop pattern.

NOMENCLATURE

A flow-path area
L axial length of a blade row
U pitchline blade rotational speed, ωr
a local speed of sound
e_0 total internal energy
f body force per unit volume
p pressure
r_m pitchline radius
u axial component of flow velocity
v_θ circumferential component of flow velocity
$\dot{w}_s$ shaft power per unit volume
ρ density
ϕ flow coefficient, u/U
ψ_f body force coefficient
$()_x$ axial component
$()_\theta$ circumferential component

Introduction

There is a continuous push to increase the performance, efficiency and operational envelope of gas turbine engines. The motivation may be application dependent, such as economy for commercial aircraft and mission requirements for military, or

*Corresponding Author

more universal in nature, such as engine response in an emergency. The design of a compressor plays a crucial role in the attainment of the overall engine goals. In particular, the operating range of a compressor significantly impacts the transient response of a gas turbine engine. At its low mass flow rate end, the operating range of a compressor is limited by aerodynamic instabilities, rotating stall and surge. Identified as separate phenomena as early as 1953 [1], the two instabilities are frequently coupled, with rotating stall typically preceding surge.

A key compressor design and development challenge is the prediction of the compressor surge line, a locus of the points on a compressor map that denote onset of either instability. In particular, there is a significant uncertainty associated with the surge line, due to both operational and modeling factors. The operational factors such as thermal and speed transients, inlet distortion and degraded tip-clearances, all erode the available surge margin. The uncertainty in stall/surge onset is largely mitigated by a conservative stall margin, enforced via acceleration limits built into the engine control system. In order to improve engine performance, efficiency and useful operating life, it is necessary to reduce the uncertainty associated with the surge line. Along with higher fidelity models, this requires improvements in the techniques employed for engine and/or rig test data analysis.

Early research on compressor stall was motivated by the issue of unrecoverable stall: A rotating stall mode that necessitates engine shutdown before return to normal operating conditions. Greitzer [2, 3] formulated the B-parameter in order to determine the preferred mode of instability in a compression system. Moore and Greitzer were the first to publish a model for compressor post stall transients [4, 5]. On the basis of the Moore-Greitzer (MG) model, Epstein et al. [6] evaluated the benefits of active control of compressor aerodynamic instabilities. They postulated that a low bandwidth control system was sufficient to suppress stall at its inception. Whereas this spurred numerous research efforts on stall control, Day [7], followed by Camp and Day [8] established an alternate stall mode. This "spike" stall inception mechanism is not predicted by the Moore-Greitzer model and hence could not be suppressed via the derived active control schemes based.

Several of the assumptions in the Moore-Greitzer model have been relaxed by researchers over the years. A review of the basic theory and some of the extensions is available in a paper by Longley [9]. Willems and de Jager [10] have also reviewed some of the extensions to the basic MG model, including the applicability to centrifugal compressors.

Whereas the Moore-Greitzer model can capture certain aspects of the overall compression system, the underlying assumptions preclude an ability to investigate inter-stage dynamics. An alternate approach replaces the blade rows with compact or distributed source terms. This "body force" approach can be used to explicitly study the inter-stage and inter-row dynamics. Sugiyama et al. [11] have used the "body force" method as part of a transient simulation of the J85 engine. Hosny et al. [12] proposed an active stabilization method, using stator dithering as the control input, that used the body force formulation. Hale and Davis [13] have presented the details of a comprehensive dynamic compressor code, called DYNTECC, that also uses the body force approach. To date, the body force method has only been used to capture 1D axial perturbations. The effect of the rotating stall is captured by a judicious use of source terms that reflects the loss of pumping capability of a stage. Recent work by Nakano and Breeze-Stringfellow [14] highlights the importance of individual stage characteristics on the overall compression system stability. In particular, this work shows that a destabilizing rear stage can overcome the positive contributions of stabilizing front stages, leading to compression system instability. Although the importance of the steady state stage matching has been well known, this work emphasizes the need for a deeper understanding of the dynamic interaction between compressor stages.

This paper describes a 1D numerical simulation model that has been developed to investigate the impact of stage characteristics, as well as load distribution on the compression and expansion waves that develop prior to a surge event. Through a controlled weakening of selected stages, the time evolution of these waves is related back to the stalling stage. It is emphasized that the formulation used in this work is not necessarily different from some of those developed by earlier researchers. The novelty is in the application of a combination of existing approaches that yields a different perspective to the compressor stalling dynamics. A goal of this paper is to provide a working recipe of the developed model. A key contribution of this work is the delineation of weak and stalling stages. In particular, it is shown that an under-performing stage can potentially cause another stage to stall. The resulting pattern of compression-expansion waves would only reflect the symptom, and not the root cause of any unexpected compression system instabilities. Whereas this may not necessarily be a new fact for experienced compressor designers, its demonstration via analysis of a simple compression system model has not been found in existing literature.

It may be noted that given the 1-D nature of the model described, no distinction can be made between rotating stall or surge. In the sequel both stall and surge are used interchangeably to denote compression system instability.

Compression System Model

The compression system studied in the present work is representative of a typical laboratory or rig-test setup. A schematic of the system under consideration is presented in Figure 1. An inlet duct feeds the compressor, which discharges into a plenum via an exhaust duct. The compressor is assumed to be externally driven and hence operating at a constant rotational speed. A throttle valve downstream of the plenum sets the operating point of the system. In particular, the closing and opening of the

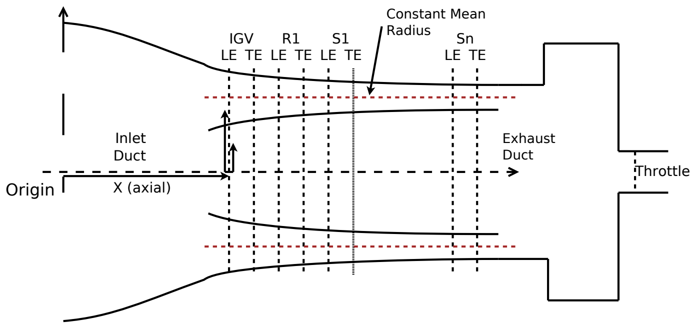

FIGURE 1. A schematic of a basic compression system test rig.

throttle respectively loads and unloads the compression system. The E^3 compressor [15] has been used as the basis of model development. Whereas the choice is motivated by the availability of its detailed design, the phenomena of interest are present in any multi-stage compressor.

The intent is to develop a simulation tool that can be used to understand and visualize the impact of stage characteristics on expansion and compression waves observed in a compression system at and after stall onset. The stage characteristics of the E^3 compressor are not available in the published literature. However, Luxin et al. [16] have applied a stage stacking approach to the published data in order to estimate the individual stage characteristics. It is recognized that the accuracy of characteristics estimated in this fashion may not be sufficient for the investigation of a specific machine. Still, they are expected to yield physically relevant trends and it should be possible to draw conclusions that are relevant to compressor designs in general. Further, it may be noted that given sufficient geometry and characteristics information, the model can be refined for a particular compressor.

Governing Equations In order to meet the stated objectives, a blade row can be replaced by a duct of varying cross-sectional area with force and work source terms, as appropriate. The source terms model the force and energy imparted by the blade row to the working fluid. The flow is assumed to be inviscid, unsteady, compressible and axisymmetric. An implication of the axisymmetric assumption is that the model cannot exhibit circumferential modes and hence cannot capture rotating stall. However, the loss of blade forcing due to rotating stall can be included by choosing the right form of the source terms for the affected blade row. Similarly, the viscous and other losses are also included within the source terms. Consequently, the correct determination of the source terms is crucial to the ability of the model to capture the observed physical behavior.

Within the stated assumptions, the general 3-D Navier Stokes equations reduce to the pseudo 1-D Euler system of equations with body force and shaft power terms. The set of equations includes the effect of area variation along the axial direction. The turning of the flow by both the rotor and stator rows implies that, even for axisymmetric flow, the circumferential momentum varies along the length of the compressor. Consequently, the set of equations also includes the circumferential component of the momentum equation.

The system of equations, continuity, momentum and energy conversation, can be written as,

$$\begin{aligned}
\frac{\partial}{\partial t}(\rho A) \quad &+\frac{\partial}{\partial x}(\rho u A) &&= 0 \\
\frac{\partial}{\partial t}(\rho u A) \quad &+\frac{\partial}{\partial x}[(p+\rho u^2)A] &&= f_x A + p\frac{\partial A}{\partial x} \\
\frac{\partial}{\partial t}(r_m \rho v_\theta A) \quad &+\frac{\partial}{\partial x}[(r_m \rho u v_\theta)A] &&= f_\theta A r_m \\
\frac{\partial}{\partial t}(\rho e_0 A) \quad &+\frac{\partial}{\partial x}[(\rho e_0 + p)uA] &&= \dot{w}_s A
\end{aligned} \tag{1}$$

Assuming that the mean radius (pitchline) is constant, the angular momentum equation can be expressed as,

$$\frac{\partial}{\partial t}(\rho v_\theta A) + \frac{\partial}{\partial x}[(\rho u v_\theta)A] = \quad f_\theta A$$

It is emphasized that the constant pitchline assumption does not restrict the validity of the results presented here. First, compressor designs with nearly constant pitchline exist, and the results are directly applicable. Second, the axial variation of pitchline introduces a source term in the circumferential momentum equation. As a result, the stages of a compressor with identical characteristics but with pitchline variation, would be slightly differently matched at a given speed. Features similar to those illustrated by the simulation results would still be observed in such a compressor, perhaps under different operating conditions.

It may be noted that the second source term in the axial momentum equation is the so called area change term. Experience shows that this term is non-negligible, especially in the front stages where the annular area changes rapidly with respect to the axis of the compressor.

Source Terms As mentioned previously, the correct evaluation of the source terms is imperative in order to reasonably capture the observed compression system behavior. One way to calculate these terms, under steady conditions, is to set the time derivatives in the Euler equations to zero. The unknown sources for a given finite control volume can then be calculated using the known values of the variables at the inlet and outlet faces. Typically, this volume encompasses a stator or rotor row. If the data are only available at the stage level, a knowledge of the flow turning angles can be used to estimate the corresponding intra-stage values.

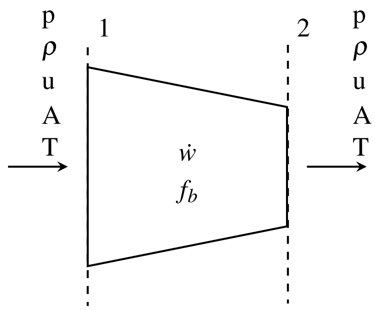

FIGURE 2. An elemental control volume. A control volume may span an entire stage, a blade row, or a part of the blade row/inter row free space.

In order to calculate the axial component of the momentum source terms, consider a finite volume illustrated in Fig 2. The application of steady state force balance to this volume leads to the following expression for the body force term,

$$f_x \frac{A_1+A_2}{2} L = (p_2A_2 - p_1A_1) + (\rho_2 u_2^2 A_2 - \rho_1 u_1^2 A_1) - \frac{p_1+p_2}{2}(A_2 - A_1)$$

Using the flow continuity, this can be reduced to

$$f_x \frac{A_1+A_2}{2} L = (p_2 - p_1)\frac{A_1+A_2}{2} + \rho_1 u_1 A_1 (u_2 - u_1)$$

A characteristic coefficient for the axial body force force per unit volume may be defined as,

$$\begin{aligned} \psi_{f_x} L &:= \frac{f_x L}{\frac{1}{2}\rho_1 U^2} \\ &= \frac{p_2 - p_1}{\frac{1}{2}\rho_1 U^2} + 2\phi_1 \frac{2A_1}{A_1+A_2}(\phi_2 - \phi_1) \end{aligned}$$

The source terms in the circumferential momentum equation are due to both the rotor and stator induced flow turning. These can be calculated along the same lines as their axial counterpart. Specifically, for a constant mean radius, the steady state momentum balance yields,

$$\begin{aligned} f_\theta \frac{A_1+A_2}{2} L &= (\rho_2 u_2 A_2 v_{\theta 2} - \rho_1 u_1 A_1 v_{\theta 1}) \\ &= \dot{m}(v_{\theta 2} - v_{\theta 1}) \end{aligned}$$

and the characteristic circumferential force coefficient can be expressed as,

$$\begin{aligned} \psi_{f_\theta} L &:= \frac{f_\theta L}{\frac{1}{2}\rho_1 U^2} \\ &= 2\phi_1 \frac{2A_1}{A_1+A_2}(\phi_2 \tan\alpha_2 - \phi_1 \tan\alpha_1) \end{aligned}$$

Finally, a consideration of steady state energy balance yields,

$$\dot{w}_s L := \dot{m} \frac{2}{A_1+A_2} \Delta h_0$$

where $\dot{w}_s$ is the shaft power per unit volume. For the rotor row, the circumferential body force and work are related through,

$$\dot{w}_s = f_\theta U$$

The form of the terms on the right in the expressions above is probably familiar to most researchers. Work and pressure coefficients are fundamental characteristics of any stage. Thus the expressions above show that the shaft power and body force terms are also characteristics of a stage.

It is generally accepted that a first order lag equation relates the unsteady force term to its steady counterpart. The unsteady body force is then given by,

$$\tau \frac{d}{dt} f_{unsteady} + f_{unsteady} = f_{steady}$$

As the work is a consequence of the forces, it may be appropriate to assume a similar relationship between unsteady and steady shaft power source terms.

Numerical Scheme A variety of numerical schemes have been developed over the years that can be applied to problems governed by conservative laws. A generic conservative law with source terms can be written as,

$$\frac{\partial}{\partial t} u(x,t) + \frac{\partial}{\partial x} f(u) = q(u) \quad (2)$$

Where $u(.)$ is the conserved variable, $f(.)$ is the flux, and $q(.)$ is a source term.

An in-depth discussion of numerical methods for fluid dynamics is beyond the scope of this paper. Briefly, the numerical methods can be classified as finite difference or finite volume methods. The finite volume methods are generally considered to be more suitable for flows where a discontinuity may arise. The numerical schemes may also be classified as upwind schemes and central difference schemes. Although the upwind schemes are generally superior in terms of lower numerical dissipation and higher accuracy, they require an exact or approximate Riemann solver, adding to their complexity. The upwind schemes are also considered to be more aligned with the flow physics. Traditionally, the central schemes tend to be more dissipative than upwind schemes. However, the recent improvements in central difference schemes have significantly improved their ability to correctly capture flow discontinuities.

The Lax-Friedrichs (LxF) is one of the earliest central difference schemes. Nessyahu and Tadmor [17] (NT) proposed a modification of the basic LxF scheme to improve its accuracy as well as lower the numerical viscosity. Building on the NT scheme, Kurganov and Tadmor [18] introduced a central difference approach with even lower numerical viscosity. A key aspect of the Kurganov-Tadmor (KT) scheme is the existence of the semi-discrete variant, where the original partial difference equation is transformed into an ordinary differential equation (ODE). It is typically easier to incorporate source terms in a semi-discrete numerical scheme. The resulting ODE can be solved via any standard ODE solver. In particular, the family of Runge-Kutta solvers has been found to be suitable for this purpose. The modern central difference schemes retain one of the key advantages of the LxF scheme, they do not require the construction of a Riemann Solver.

Numerical schemes can be compactly expressed if it is assumed that the computational grid is uniformly spaced. However, where the compressor is concerned, it is more natural to place grid points at the inlet and outlet of blade rows, leading to a non-uniformly spaced grid. Consequently, the KT semi-discrete scheme has been adapted to a non-uniform grid. For a conservative law of Eqn. 2, the semi-discrete form for a non-uniform grid is given by,

$$\frac{d}{dt}u_j(t) = -\frac{H_{j+\frac{1}{2}}(t) - H_{j-\frac{1}{2}}(t)}{\Delta x_{j,c}} + q(u_j(t))$$

The numerical flux, H, can be expressed as,

$$H_{j+\frac{1}{2}}(t) = \frac{f(u^+_{j+\frac{1}{2}}) + f(u^-_{j+\frac{1}{2}})}{2} - a_{j+\frac{1}{2}}\frac{u^+_{j+\frac{1}{2}}(t) - u^-_{j+\frac{1}{2}}(t)}{2}$$

where the value of the conserved variable u due to left and right traveling waves is given by,

$$\begin{aligned} u^+_{j+\frac{1}{2}} &= u_{j+1}(t) \quad -u_{x_{j+1}}(t)\frac{\Delta x_{j+1,c}}{2} \\ u^-_{j+\frac{1}{2}} &= u_j(t) \quad +u_{x_j}(t)\frac{\Delta x_{j,c}}{2} \end{aligned}$$

For a non-uniform grid, both central and one-sided deltas are required. Specifically,

$$\begin{aligned} \Delta x_{j,c} &= \frac{x_{j+i} - x_{j-1}}{2} \\ \Delta x_j &= x_{j+i} - x_j \end{aligned}$$

with

$$\begin{aligned} \Delta u_{x_j} &= minmod(\theta\frac{u_j - u_{j-1}}{\Delta x_{j-1}}, \frac{u_{j+1} - u_{j-1}}{2\Delta x_{j,c}}, \theta\frac{u_{j+1} - u_j}{\Delta x_{j+1}}) \\ & 1 \le \theta \le 2 \\ a_{j+\frac{1}{2}} &= \text{maximal local speed of sound} \end{aligned}$$

The parameter θ affects the dissipation of the scheme, with $\theta = 2$ corresponding to the least dissipative formulation. A value of 1.8 has been used in the present work.

Although the central schemes tend to be more dissipative than upwind schemes, the simulation of the "shock tube" problem using the KT central scheme shows that it can accurately capture the normal shock as well as the contact surface [18]. Consequently, the KT central difference scheme is considered to be suitable for present work.

Simulation Studies

Georgia Tech has pioneered a compressor stability measure, called the correlation measure, that is sensitive to local stage stability [19]. Experience with this measure suggests that a weaker stage, one that exhibits sub-par performance can cause a different stage to stall. A hypothetical 3-stage compressor has been simulated in order to investigate this phenomenon. Of particular interest is the role of the degraded stage on the stall process. This hypothetical compressor comprises the first 3 stages of the E^3-compressor operating at design speed.

At the start of the simulated test, the compressor is operating near its stall point. A milli-second into the run, the exit throttle is closed by a fixed amount in a single step. The plenum acts as a filter, converting the step input into a ramp like increase in the back pressure. Depending on the case, the compressor stalls 3ms to 6ms into the run. Results are presented in the form of static pressure and axial velocity time traces. Static pressure probes are typically the only instrumentation located in-between stages. Frequently, a stalling stage is identified by a sharp pressure rise upstream of it and a corresponding pressure drop downstream. The axial velocity or local mass flow rate, if available, would be a better indicator of a stalling stage. Results for both pressure and velocity are presented to illustrate the correlation, or lack there of, between the trends observed in each case.

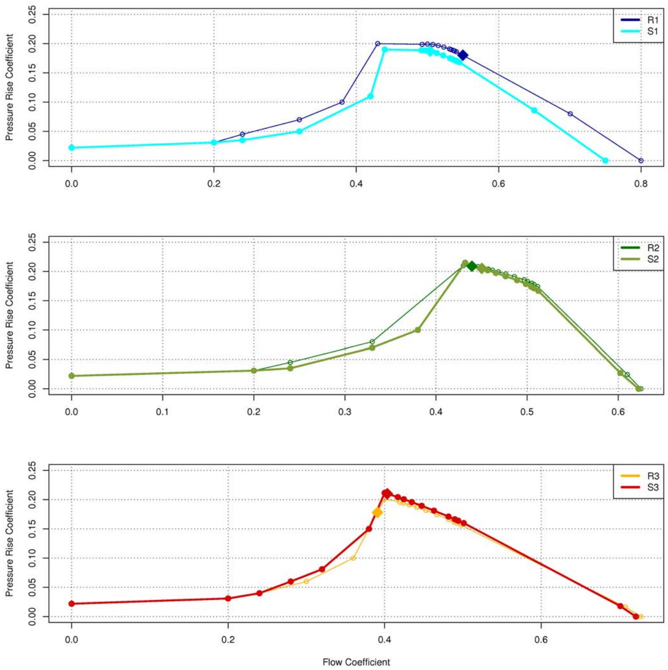

FIGURE 3. The nominal stage characteristics of hypothetical 3-stage compressor. The solid diamond symbols mark the position on the stage characteristics that corresponds to stall onset (dashed vertical line in Fig. 4).

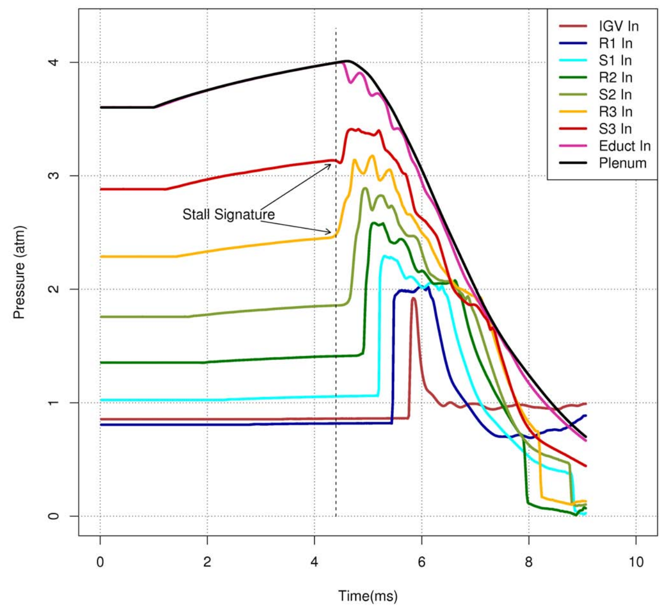

FIGURE 4. Pressure time history when the nominal compressor is throttled into stall. First noticeable change to the gradual pressure rise can be observed in the pressure jump at the inlet to the 3rd rotor.

It is emphasized that due to the 1-D nature of the simulated model, rotating stall cannot be explicitly captured. Both stall and surge in the context of this model denote the onset of global compression system instabilities.

Nominal Response The nominal pressure-velocity coefficient characteristics are shown in Fig. 3. As noted, the solid diamond symbols identify the operating point on the particular characteristic that corresponds to the stall onset of the entire system. It may be observed from the pressure traces in Fig. 4 that the compression system stalls 4ms into the run. The first sign of trouble in the pressure traces is a sharp pressure rise at the inlet of the 3rd rotor. A nearly simultaneous jump in the pressure at the inlet to the downstream stator can also be observed, along with a drop in pressure at its exit. The usual interpretation would suggest that the 3rd stage has stalled, leading to a global system instability.

It may be noted that although the small drop in the pressure at the inlet to the 3rd stage stator is visible in the simulated results, it is unlikely that a drop of this magnitude would be captured in experimental data. In principle, frequency analysis of fast response pressure sensor can isolate the start of this expansion wave. However, experience shows that real-life signals contain a range of frequencies and it is not trivial to separate signal from noise without prior knowledge of frequencies of interest.

An investigation of the flow velocities also shows a similar trend. The flow velocities at each station vary gradually, decreasing till the system stalls. The first break in the smooth trend can be observed in the velocity at the inlets to the stage 3 rotor and stator (Fig. 5). A re-evaluation of Fig. 3 also shows that at the stall onset, stage 1 and 2 are operating in the negatively inclined portion of the respective characteristics. Stage 3 rotor is the first row where the operating point moves to the positively sloped portion of the characteristics.

Wider Operating Stage As the 3rd stage was deemed to be the stalling stage, the next case incorporates a wider operating 3rd stage. The first two stages remain unchanged. The characteristics of the improved compressor are shown in Fig. 6. The unstalled behavior of this system is nearly identical to the nominal compressor. Analysis of the pressure time traces presented in Fig. 7 indicates that the 2nd stage may be the stalling stage. The first pair of compression and expansion wave can be observed upstream and downstream respectively of the 2nd stator. The instability quickly spreads to the entire machine. It may be noted that the overall pressure ratio of the machine at stall is similar to that of the nominal compressor. This suggests that

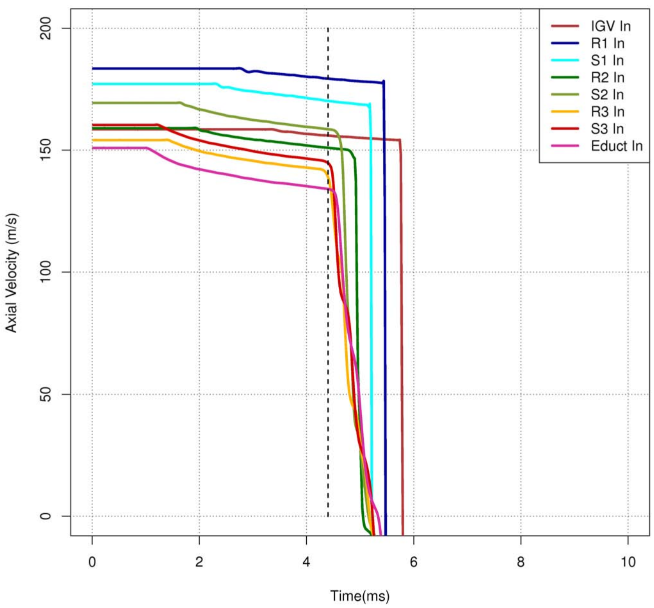

FIGURE 5. Axial flow velocity time history when the nominal compressor is throttled into stall. The sharp drop in the velocity at the 3rd rotor and stator is consistent with the pressure waves emanating from the two rows.

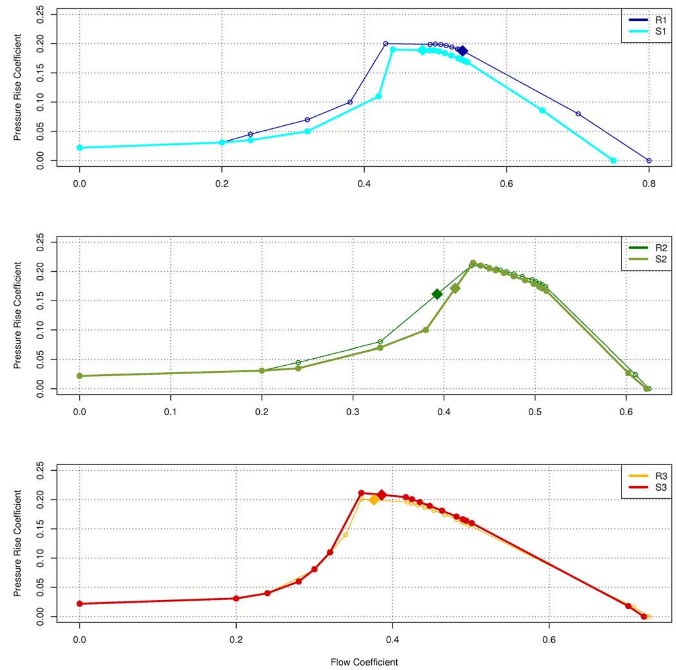

FIGURE 6. Stage characteristics for the hypothetical 3-stage compressor where the 3rd stage has a higher operating range. The solid diamond symbols mark the position on the stage characteristics that corresponds to stall onset (dashed vertical line in Fig. 7).

improving a single stage may not yield any benefit at a global, system level.

The transient behavior of the axial velocities is not entirely consistent with the observations made using the pressure time traces. As evident in Fig. 8, the first noticeable change in the axial flow velocity occurs at the inlet to the 2nd rotor (dark green), and precedes the drop in the flow velocity at the inlet to the 2nd stage stator (olive). The drop in the stator's inlet velocity is aligned with the dashed vertical marker, whereas the flow velocity at the rotor inlet starts dropping approximately 0.5ms before the marker. The stage characteristics (Fig. 6) show that at the point of stall onset, both the rotor and stator of the 2nd stage were operating at the positive sloped portion of their respective characteristics.

Weak Stage A third scenario consists of a significantly weaker 2nd stage coupled with nominal 1st and 3rd stages. It may be natural to expect that the 2nd stage would be the stalling stage for such a compressor, however the simulated test shows a murkier picture. The characteristics of the three stages are shown in Fig. 9. The second stage characteristic is nearly symmetric around the peak pressure rise point, and gently transitions from negative to positive slopes. The nominal 2nd stage is negatively sloped till flow coefficient is reduced to 0.43. Its weaker counterpart has a positive sloped characteristic for flow coefficients less than 0.46. This is a significant reduction in the performance of a stage.

The pressure traces for a compressor with weakened 2nd stage are shown in Fig. 10. The first significant sign of a sharp pressure-rise can be seen at the inlet to the 3rd stator. This would lead one to conclude that the 3rd stage is the first to stall.

The stall sequence picture is not really clarified by the axial velocity transients. As seen in Fig. 11, the drop in flow velocities is nearly simultaneous across the 2nd and 3rd stage rows, with the 2nd stage rows slightly preceding the 3rd row. The operating point of the three stages relative to their characteristics at stall onset, marked in Fig. 9, illustrates the issues with concluding that the 3rd stage is the stalling stage. Both the rows of the 2nd stage are operating well into the positively sloped portion of the respective characteristics. On the other hand, the 3rd stage operating point is just to the left of the peak in its characteristics. Further, in this controlled experiment, the 2nd stage was deliberately weakened and it would be natural to expect that it would lead to eventual system instabilities.

In essence, the simulated results show that upto a point, the destabilizing 2nd stage is countered by the stabilizing 1st and 3rd stages. The global instability is initiated when the 3rd stage

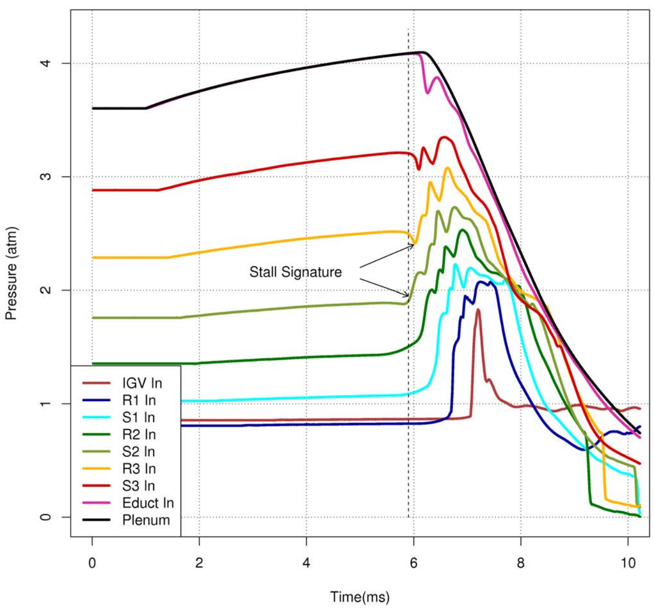

FIGURE 7. Pressure time history when the improved compressor is throttled into stall. First noticeable change in the gradual pressure rise can be observed in the pressure at the inlet to the 2nd stator.

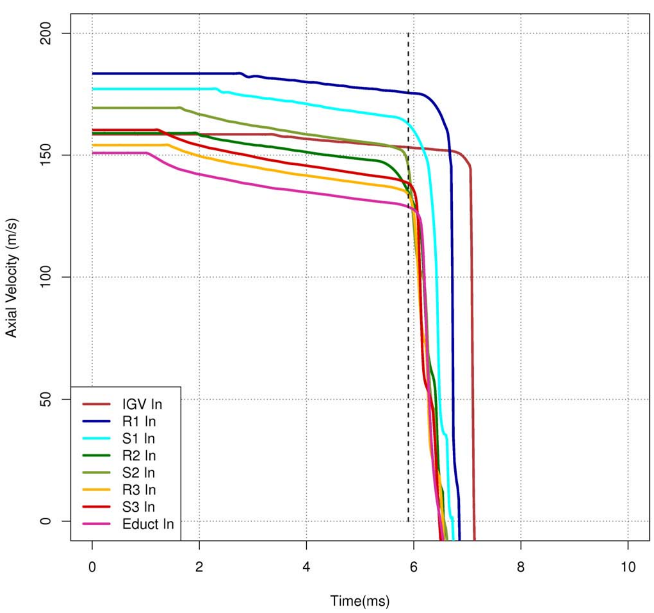

FIGURE 8. Axial flow velocity time history for the compressor with an improved 3rd stage. The sharp drop in the velocity at the 2nd rotor is not completely consistent with the pressure waves emanating from the same location.

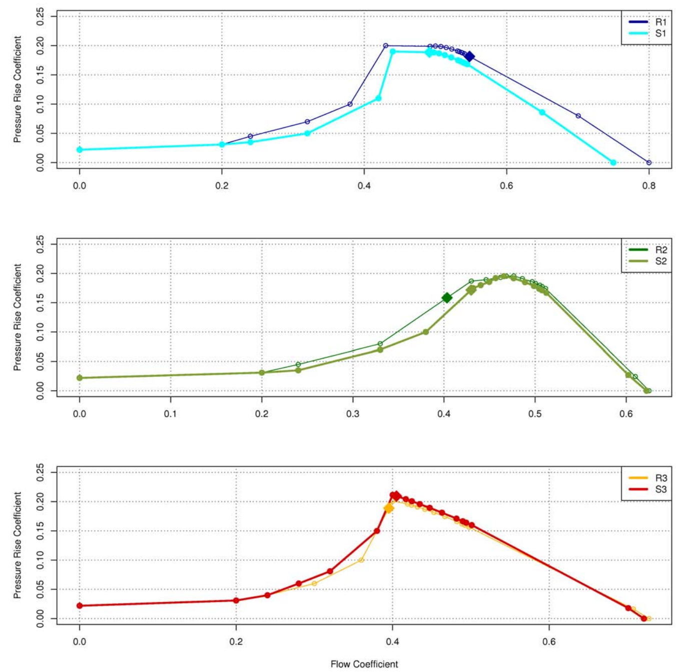

FIGURE 9. Stage characteristics for the hypothetical 3-stage compressor where the 2nd stage is weaker than normal. The solid diamond symbols mark the position on the stage characteristics that corresponds to stall onset

is unable to sustain the higher loading necessary to offset the loss of pumping of the 2nd stage. It is emphasized that the simulated 3-stage compressor comprises of the first 3 stages of the E^3 compressor and is not a well matched 3-stage compressor. However, the results observed here are applicable to a general multi-stage compressor. In particular, a weak or under-performing stage leads to a re-matching of the entire machine and can trigger a nominal stage into stalling the overall compression system.

Summary

This paper describes a 1D numerical simulation model that has been developed to investigate the impact of stage characteristics, as well as load distribution on the compression and expansion waves that develop prior to a surge event. The formulation used in this work is similar to that used by prior researchers.

Analysis of a hypothetical compressor highlights the challenges in identifying a stalled stage based on static pressure time traces. In addition, results show that a weak stage may not be the first stage to stall. In essence, the loss of performance of a particular stage leads to a re-matching of the entire compressor. The stage that eventually stalls may not be the one that is weaker than its design. It may be concluded that the pattern of compression-expansion waves only reflects the symptom, and

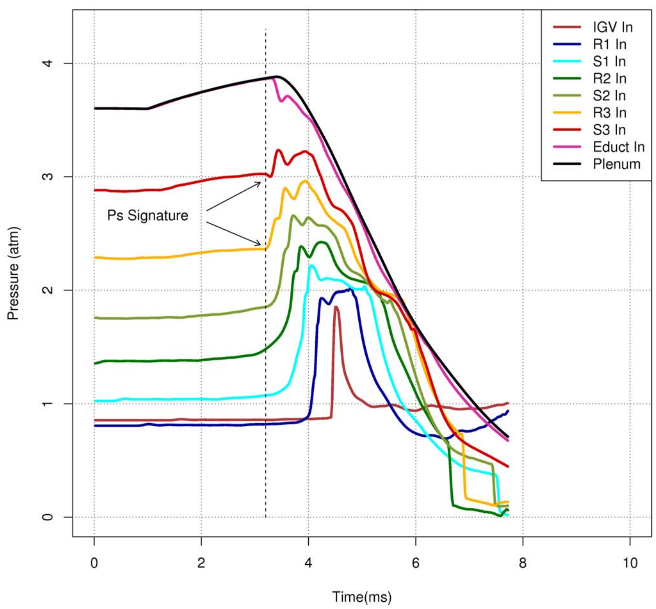

FIGURE 10. Pressure time history for the case when the compressor with weaker 2nd stage is throttled into stall. The compression and pressure wave pattern indicates that the 3rd stator may have been the first to stall.

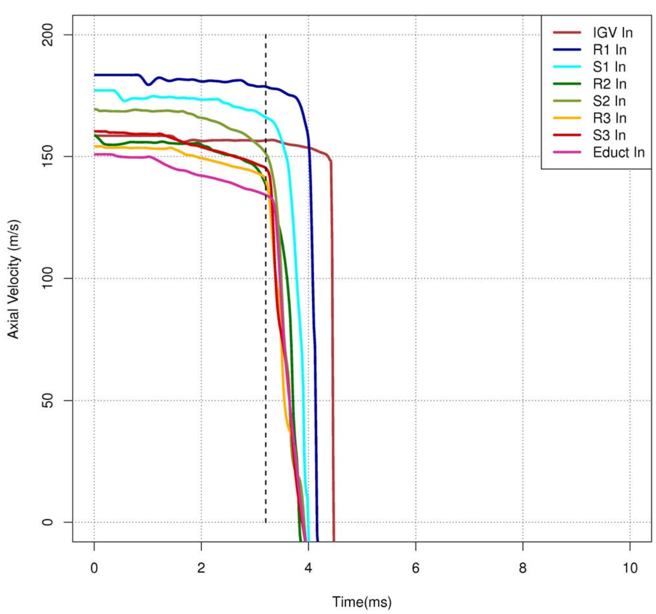

FIGURE 11. Axial flow velocity time history when the degraded compressor is throttled into stall. The local flow velocity drops simultaneously at 2nd and 3rd blade rows.

not the root cause of any unexpected compression system instabilities.

For a compressor designer the two questions: "Which stage should I improve?" and "Which stage stalled first?" are not necessarily related. Further, the results presented here highlight that the improvements to a single stage may not yield a significant overall benefit.

The model developed and utilized in this paper only considers the axial flow perturbations. Although the rotating modes cannot be explicitly modeled via the pursued approach, the effect of rotating stall can be implicitly included via an appropriate choice of source terms. In particular, the time-averaged loss of pumping due to stall is reflected in the sharp positive slope of a stage characteristic to the left of its nominal stall point. However, a quasi 1D formulation cannot be used to study the dynamic interaction between rotating and axial modes of a compressor. A coupling between the rotating stall cells and 1D axial waves can potentially affect the static pressure signature, compounding the analysis of the compressor stall sequence.

Future work will explore the possibility of directly incorporating circumferential perturbations. A goal of this work has been to produce a numerical simulation that runs quickly and hence enables a designer to carry out trade studies. It is expected that a 2D model would be computationally more expensive. The basic framework allows for simulating non-adiabatic flow via use of heat source/sink terms. A possible extension is to incorporate heat addition in the plenum and hence simulate a gas turbine combustor.

Acknowledgments

A part of this work was funded by GE Global Research Center and the support gratefully acknowledged.

REFERENCES

[1] Emmons, H., Pearson, C., and Grant, H., 1953. "Compressor surge and stall propagation". In American Society of Mechanical Engineers – Meeting A-65, Nov 29-Dec 3 1953, American Society of Mechanical Engineers – Papers, American Society of Mechanical Engineers (ASME), p. 13.

[2] Greitzer, E., 1976. "Surge And Rotating Stall In Axial Flow Compressors - 1. Theoretical Compression System Model.". *Journal of Engineering for Power, Transactions ASME,* ***98 Ser A***(2), pp. 190–198. Compendex.

[3] Greitzer, E., 1976. "Surge And Rotating Stall In Axial Flow Compressors - 2. Experimental Results And Comparison With Theory.". *Journal of Engineering for Power, Transactions ASME,* ***98 Ser A***(2), pp. 199–217. Compendex.

[4] Moore, F., and Greitzer, E., 1986. "Theory Of Post-Stall Transients In Axial Compression Systems: Part i - Devel-

opment Of Equations.". *Journal of Engineering for Gas Turbines and Power,* ***108***(1), pp. 68–76. Compendex.

[5] Greitzer, E., and Moore, F., 1986. "Theory Of Post-Stall Transients In Axial Compression Systems: Part Ii - Application.". *Journal of Engineering for Gas Turbines and Power,* ***108***(2), pp. 231–239. Compendex.

[6] Epstein, A., Williams, J., and Greitzer, E., 1989. "Active suppression of aerodynamic instabilities in turbomachines". *Journal of Propulsion and Power,* ***5***(2), pp. 204–211. Compendex.

[7] Day, I., 1993. "Stall inception in axial flow compressors". *Journal of Turbomachinery,* ***115***(1), pp. 1–9. Compendex.

[8] Camp, T., and Day, I., 1998. "A study of spike and modal stall phenomena in a low-speed axial compressor". *Journal of Turbomachinery,* ***120***(3), pp. 393–401. Compendex.

[9] Longley, J., 1994. "Review of nonsteady flow models for compressor stability". *Journal of Turbomachinery,* ***116***(2), pp. 202–215. Compendex.

[10] Willems, F., and Jager, B. D., 1999. "Modeling and control of compressor flow instabilities". *IEEE Control Systems Magazine,* ***19***(5), pp. 8–18. Compendex.

[11] Sugiyama, Y., Tabakoff, W., and Hamed, A., 1989. "J85 surge transient simulation". *Journal of Propulsion and Power. Vol. 5,* ***5***, pp. 375–381. Proceedings, p. 568-578; Previously cited in issue 20, p. 3161, Accession no. A87-46240.

[12] Hosny, W., Leventhal, L., and Steenken, W., 1991. "Active stabilization of multistage axial-compressor aerodynamic system instabilities". American Society of Mechanical Engineers (Paper), Publ by ASME, New York, NY, USA, p. 8.

[13] Hale, A. A., and Davis, M. W., 1992. "DYNamic turbine engine compressor code (DYNTECC) - theory and capabilities". *AIAA*, pp. 6–8. Research supported by USAF.

[14] Nakano, T., and Breeze-Stringfellow, A., 2011. "A method for evaluating the aerodynamic stability of multistage Axial-Flow compressors". *Journal of Turbomachinery,* ***133***(3), July, pp. 031004–11.

[15] Holloway, P. R., Knight, G. L., Koch, C. C., and Schaffer, S. J., 1982. Energy efficient engine: High pressure compressor - detailed design report. Contractor Report 165558, National Aeronautics and Space Administration.

[16] Luxin, L., Neumeier, Y., and Prasad, J. V. R., 2005. "Active flow control for enhanced compressor performance". *41st AIAA/ASME/SAE/ASEE Joint Propulsion Conference & Exhibit*, pp. 10–13.

[17] Nessyahu, H., and Tadmor, E., 1990. "Non-oscillatory central differencing for hyperbolic conservation laws". *Journal of Computational Physics,* ***87***(2), Apr., pp. 408–63. Copyright 1990, IEE.

[18] Kurganov, A., and Tadmor, E., 2000. "New high-resolution central schemes for nonlinear conservation laws and convection-diffusion equations". *Journal of Computational Physics,* ***160***(1), May, pp. 241–82. Copyright 2000, IEE.

[19] Dhingra, M., 2006. "Compressor stability management". PhD thesis, Georgia Institute of Technology, Atlanta, GA, USA.